Journal of Materials Chemistry A

ROYAL SOCIETY OF CHEMISTRY

COMMUNICATION

View Article Online
View Journal | View Issue

Cite this: J. Mater. Chem. A, 2023, 11, 16003

Received 2nd March 2023
Accepted 20th July 2023

DOI: 10.1039/d3ta01284k

rsc.li/materials-a

Effect of singlet oxygen on redox mediators in lithium–oxygen batteries†

Hyun-Wook Lee, [ab] Ja-Yeong Kim,[ab] Joo-Eun Kim,[b] Yun-Joo Jo,[b] Daniel Dewar, [c] Sixie Yang,[c] Xiangwen Gao,*[c] Peter G. Bruce *[c] and Won-Jin Kwak *[ab]

The use of a redox mediator (RM) to chemically decompose Li_2O_2 is an efficient approach to improve the efficiency and cyclability of lithium–oxygen batteries. It has been suggested that RMs can react with the singlet oxygen ($^1O_2$) but no attempt has been made to categorize the reactivity of different RMs with $^1O_2$, or investigate the impact of this reaction on the electrochemical behavior of RMs. Here we show that the reactivity of RMs with $^1O_2$ depends on the unique chemistry of the RM, and that the Li_2O_2 decomposition kinetics of RMs are considerably affected by their reactivity towards $^1O_2$. We examine changes to the chemical and electrochemical properties of RMs after exposure to $^1O_2$. These results suggest that the activity and lifetime of RMs in Li–O_2 cells are affected by their reactivity towards $^1O_2$, and that RMs can be classified depending on how easily they react with, or physically quench $^1O_2$.

Introduction

Lithium oxygen batteries (LOBs) have been suggested as a next-generation energy storage device due to their high theoretical energy density.[1] However, the low energy efficiency and irreversibility of this system hinder its practical applications.[2–5] One characteristic drawback of LOBs is the high charging overpotential required to oxidize the insulating discharge product, lithium peroxide (Li_2O_2). This simultaneously causes electrolyte decomposition, therefore the formation of a corrosive solid–electrolyte interface layer, which lowers coulombic efficiency and deteriorates cycling performance.[6–8] To decrease the charging overpotential, various approaches, *e.g.* embedding catalysts in the cathode,[9,10] structural design of porous air electrodes,[11,12] and solvent design[13,14] have been proposed. Among them, redox mediators (RMs) are one of the most promising methods.[15–19] Instead of electrochemically oxidizing Li_2O_2, RMs themselves are oxidized first at a lower potential and the oxidized RMs chemically decompose Li_2O_2.[20] With this mechanism, RMs can effectively mitigate undesired side reactions at high voltage region and improve energy efficiency and cyclability. Singlet oxygen ($^1O_2$) has recently been identified as a reactive oxygen species in LOBs, which inevitably forms during cycling test especially in LiO_2 disproportionation reactions.[21–24] The highly reactive $^1O_2$ has been suggested to provoke side reactions by attacking the cathode, electrolyte and RMs.[25–27] For this reason, $^1O_2$ was pointed out as a major concern, and various approaches for diminishing $^1O_2$ have been studied.[27–31] It has also been reported that RMs can induce the relaxation of $^1O_2$ into $^3O_2$ by physically interacting with $^1O_2$, which is called quenching.[32,33] However, it is complicated by the possibility of either a reversible (quenching) or irreversible (trapping) reaction, both of which will scavenge $^1O_2$.[34] Contradicting reports raise the question whether the reaction of RMs with $^1O_2$ truly leads to the deactivation of RMs and yet, no direct evidence has been presented.[27,35] Therefore, classification of the reactions between RMs and $^1O_2$ is required alongside clarification on if the reaction between RMs and $^1O_2$ leads to deactivation of RMs.

In this study, we systematically investigated both the chemical and electrochemical properties of RMs after exposure to $^1O_2$ to fully understand the effect of $^1O_2$ on RMs. We find that the reaction of RMs with $^1O_2$ not only affects the chemical properties but also the electrochemical properties of RMs. Due to the unique chemistry of RMs towards $^1O_2$, RMs can be put into three categories: comparatively inactive towards $^1O_2$, chemically reactive with $^1O_2$, or a physical $^1O_2$ quencher. Moreover, changes to the electrochemical properties after exposure to $^1O_2$ have been observed and discussed.

Results and discussion

Observation of reactivity of redox mediators with $^1O_2$

Five RMs with different redox potentials, (tris[4-(diethylamino) phenyl]amine (TDPA), *N*,*N*,*N*′,*N*′-tetramethyl-*p*-phenylenedia

[a]School of Energy and Chemical Engineering, UNIST, Ulsan, 44919, Republic of Korea. E-mail: wjkwak@unist.ac.kr

[b]Department of Energy Systems Research, Ajou University, Suwon, 16499, Republic of Korea

[c]Department of Materials, University of Oxford, Oxford, UK. E-mail: xiangwen.gao@materials.ox.ac.uk; peter.bruce@materials.ox.ac.uk

† Electronic supplementary information (ESI) available. See DOI: https://doi.org/10.1039/d3ta01284k

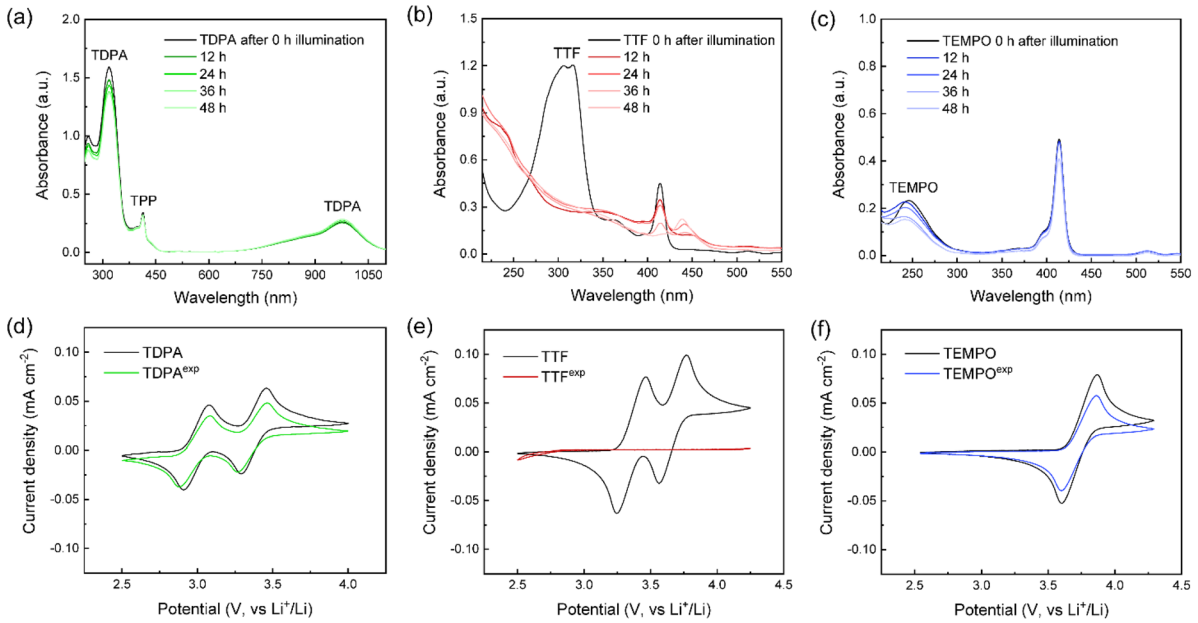

Fig. 1 Reactivity with $^1O_2$ and electrochemical redox sustainability of RMs. UV-vis spectra of (a) TDPA, (b) TTF and (c) TEMPO for every 12 hours, up to 48 hours. Electrolyte consisted of 1 M LiTFSI, 50 mM RM and 0.5 mM TPP in TEGDME, and diluted into 1/1000 scale with acetonitrile. Cyclic voltammetries (CVs) of (d) TDPA, (e) TTF and (f) TEMPO before and after 48 hours of illumination at 10 mV s^{-1} using 50 mM RM in TEGDME with 0.5 mM TPP under Ar atmosphere.

mine (TMPD), tetrathiafulvalene (TTF), 2,2,6,6-tetramethylpiperidine-1-oxyl (TEMPO) and 10-methylphenothiazine (MPT)) were chosen, where each RM has different reaction kinetics with Li_2O_2 following Marcus theory.[33,36] We aimed to expose these RMs to $^1O_2$ generated *via* photosensitizer, *meso*-tetraphenylporphine (TPP) dissolved in the solution.[37,38] To determine the $^1O_2$ evolution rate in actual cell conditions, $^1O_2$ evolved during cycling of a cell was measured with the well-known $^1O_2$ probe, 9,10-dimethylanthracene (DMA).[39–41] After discharging at 0.1 mA cm^{-2} for 5 hours, the absorbance of DMA was decreased to 81% compared to initial absorbance, indicating that DMA was consumed by $^1O_2$ evolved during discharging (Fig. S1†). Several pieces of literature have used DMA during charging[31,32,42,43] but the oxidation potential of DMA is lower than 4 V (*vs.* Li^+/Li) (Fig. S2†). Therefore DMA was not used here for charging to avoid possible ambiguity and instead approximated the amount of $^1O_2$ during charging following previous reports (more details on Discussion 1). Typically, cyclability of RMs in LOBs is measured over 50 cycles, often more than 100 cycles (Table S1†). During cycling, RMs are continuously exposed to and react with $^1O_2$. Therefore, it is necessary that a RM is resistive against $^1O_2$ to maintain its function and the low charging overpotential. In this respect, we exposed RMs to an amount of $^1O_2$ that fully simulates the RM's status after $^1O_2$ exposure.

Fig. 1 and S3† show the reactivity of various RMs with $^1O_2$ after exposure to $^1O_2$ for 48 hours. TDPA and TEMPO showed relatively small changes in the absorption spectrum compared to other RMs. TTF experienced the most drastic changes. The peak near 300 nm vanished only after 12 hours of exposure to $^1O_2$, and the peak of TPP near 420 nm kept decreasing, implying some side reactions between TPP and TTF originated byproducts. TTF has two five-membered ring structures with four sulfur atoms, where the sites near the sulfur atoms can easily react with electrophilic species, in this case, $^1O_2$.[44–46] The other two RMs, TMPD and MPT showed similar degradation with that of TTF, implying similarly poor molecular stability. Besides the chemical reactivity, the electrochemical activities of RMs after exposure to $^1O_2$ were also examined by the cyclic voltammetry (CV) profiles of each RM before and after 48 hours of $^1O_2$ exposure (RM^{exp}). The CV profile of TDPA and TEMPO showed slight changes after exposure to $^1O_2$ as shown in Fig. 1d and f. In contrast, TTF became electrochemically inert (Fig. 1e), in accord with the vanished peaks in the UV-vis spectrum. The stability of TPP by itself and in the presence of RMs was also evaluated (Fig. S4 and S5†), and changes of spectrum were much smaller than the effect of $^1O_2$ on the degradation of RMs. This indicates that any changes to the RMs by TPP were negligible and were affected by $^1O_2$ more (see Discussion 2 for more details). Additionally, the nuclear magnetic resonance (NMR) spectra of RM^{exp}s (Fig. S6†) were in agreement with the results shown in Fig. 1 and S3,† further confirming the reactivity after exposure to $^1O_2$. TDPA exhibited no apparent changes, with a small depression or split in the overall chemical shift. For TMPD, TTF and MPT, the indicative peaks for each RM (located near 7 ppm) disappeared or were considerably altered after 48 hours of $^1O_2$ exposure (Fig. S6†). The origin of the different reactivity of RMs toward $^1O_2$ is mainly related to their molecular structural differences leading to different energy barriers when RMs react with $^1O_2$ as previously reported.[27] More importantly, the results obtained from CVs indicate that the reaction of RMs with $^1O_2$ directly deteriorates the redox activity of RMs.

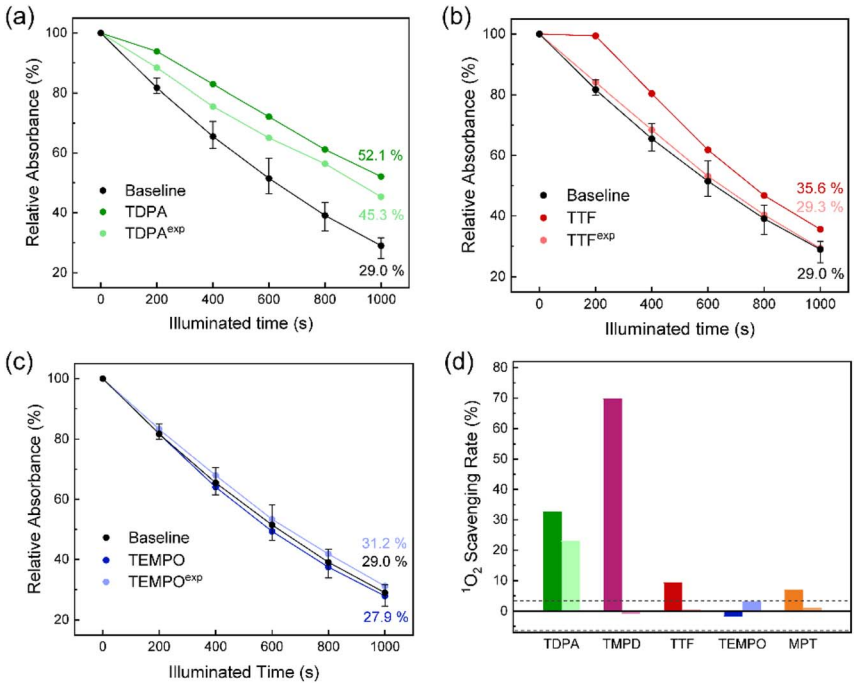

Fig. 2 $^1O_2$ scavenging efficiency of RM and RM^{exp}. Relative absorbance of DMA for 1000 s exposed to $^1O_2$ evolved by 0.3 μM of TPP with the presence of 30 μM of (a) TDPA and TDPA^{exp}, (b) TTF and TTF^{exp}, and (c) TEMPO and TEMPO^{exp} in TEGDME. 80 μM of DMA was used in initial solution stirred at 150 rpm and O_2 was purged with rate of 1 ml min^{-1}. Absorbance of DMA was measured at 379.5 nm *via* UV-Vis spectrometer. (d) $^1O_2$ scavenging rate of RMs and RM^{exp}s based on results obtained from measurement of absorbance of DMA. Bars with dark color indicates RM and bright color indicates RM^{exp}. Dashed lines are error of baseline.

Effects of $^1O_2$ on interaction between redox mediators and $^1O_2$

The $^1O_2$ scavenging ability is a major characteristic of RMs[32,33] but it is ambiguous due to the complication of reactions between RMs and $^1O_2$ as mentioned above, suggesting that the exact characterization is still required for a full understanding of the RM behavior. For this reason, not only the electrochemical redox activity, but changes in the chemical behavior of RMs before and after $^1O_2$ exposure were also examined. The route of deactivating $^1O_2$ can be classified into two different ways, trapping and quenching. Trapping means capturing $^1O_2$ in the irreversible way by chemically reacting with $^1O_2$, while quenching is the reversible physicochemical reaction, relaxing $^1O_2$ into $^3O_2$.[42,47] Trapping and quenching occurs competitively and it is difficult to investigate their individual effect with a single method. Therefore, scavenging refers both to trapping and quenching here. To examine the scavenging ability of each species, changes of DMA absorbance were measured and rescaled in relative values as shown in Fig. 2 and S7.† Each solution contained the same amount of DMA and TPP but with different RMs, and the baseline is the same solution without RM. The scavenging rate shown in Fig. 2d was calculated based on the absorbance of DMA after 1000 s of $^1O_2$ exposure and it is detailed in the ESI (Table S2†). In the TDPA-based solution, DMA maintained a 52.1% absorbance after 1000 s of exposure. Indicating the TDPA scavenging about 30% of total $^1O_2$ DMA scavenged while in TDPA^{exp}, the scavenging ability is lower with about 20% of $^1O_2$ scavenged. In contrast, the TTF-based solution showed large fluctuations in DMA absorbance because of changes to the overlapping spectrum of TTF caused by its reaction with $^1O_2$. However, TTF^{exp} showed nearly the same results as the baseline, suggesting TTF readily reacted with $^1O_2$ and lost any ability as a trap or quencher. Similarly, TMPD scavenged over 70% of $^1O_2$ but completely lost its scavenging ability after 48 hours of $^1O_2$ exposure (Fig. S7†). TEMPO, which was expected to have certain scavenging ability, exhibited no scavenging behavior and this contradicts to some previous reports.[32] Various factors such as charging potential and the morphology of Li_2O_2 formed during discharge can be considered as causes of this contradiction.

However, more importantly, DMA is electrochemically oxidized below 4 V (Fig. S2†) and therefore it might not be a suitable $^1O_2$ probe during the charging process. This can overrate the scavenging effect of a RM and make uncertainty when scavenging ability of RMs is compared. For above reason, the $^1O_2$ scavenging ability of RMs in this study were obtained *via* chemical simulation. Same with TEMPO, TEMPO^{exp} also gave none of the effect seen as scavenging, indicating scavenging ability of TEMPO is barely affected by $^1O_2$. Our results agree with other conclusions that TEMPO has a comparatively low scavenging ability compared to other RMs.[32,33] We now combine these insights with the $^1O_2$ stability against different RMs. TDPA is relatively stable towards $^1O_2$ and displays significant scavenging behavior, which identifies it as a physical quencher of $^1O_2$. TTF, TMPD and MPT showed high reactivity towards $^1O_2$ and showed decreased $^1O_2$ scavenging ability after exposure to $^1O_2$, thus identifying them as $^1O_2$ traps. TEMPO showed none of

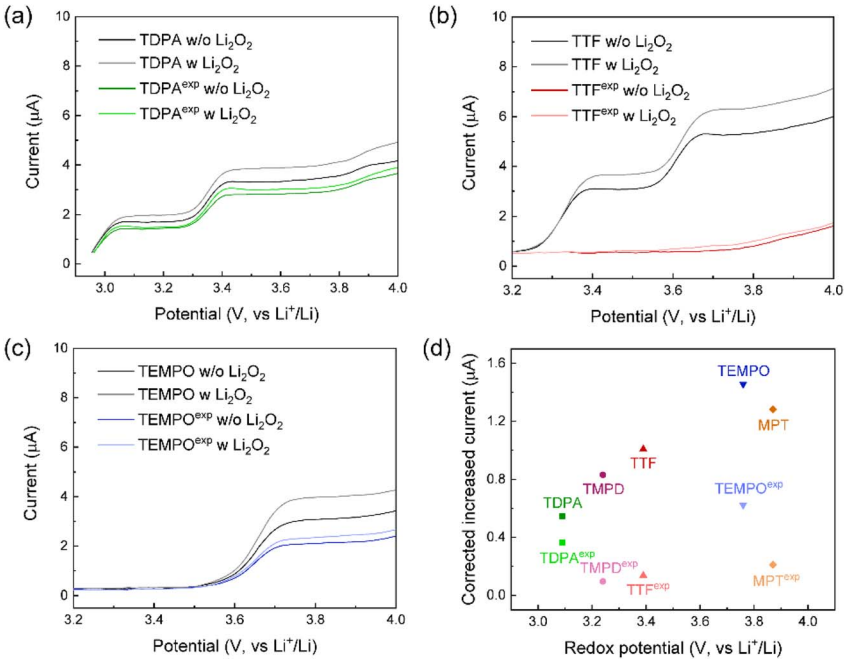

Fig. 3 Li_2O_2 oxidation kinetics of RMs and RM^{exp}s. (a)–(c) LSV curves of RMs and RM^{exp}s with or without presence of Li_2O_2 measured by LSV with rotating ring disk electrode (RRDE). (d) Kinetics of each material plotted as a function of the redox potential of each RM. RM^{exp} indicates that the RM was exposed to photocatalytically evolved $^1O_2$ for 48 hours. The increased current is calculated for the first oxidation of the RM.

quenching or trapping ability however had relatively high durability towards $^1O_2$, implying TEMPO has minimal interaction with $^1O_2$.

Li_2O_2 decomposition kinetic of redox mediators

Another fundamental characteristic of RMs is their Li_2O_2 oxidation kinetics. Changes in the kinetics after exposure to $^1O_2$ were measured by RRDE through linear sweep voltammetry (LSV) up to 4 V (*vs.* Li^+/Li)[48] and increased viscosity by Li_2O_2 addition was compensated based on Fig. 3, and S8† is the corrected increased current plotted *versus* redox potential of each RM. The overall trend in the kinetics is an inverted parabola following Marcus theory, indicating an outer-sphere electron exchange between RM and Li_2O_2. This is in agreement with previous reports performing the same experiment.[33,48] However, after exposure to $^1O_2$, the kinetics trend of the RM^{exp}s was altered significantly. LSV curves of TDPA and $TDPA^{exp}$ have two steps of Li_2O_2 decomposition (Fig. S9a†), with little change after exposure to $^1O_2$, suggesting that the kinetics of quencher-type RMs like TDPA are barely affected by $^1O_2$

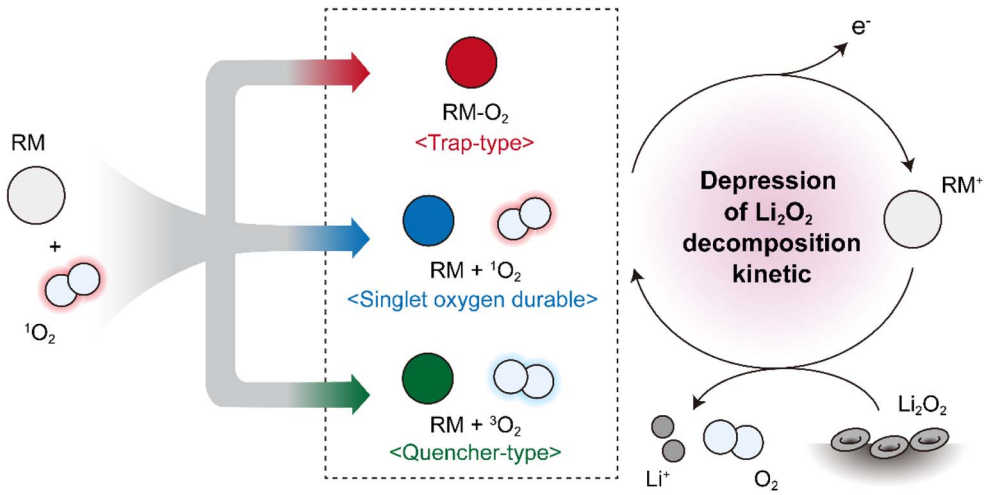

Fig. 4 Suggested classification of RMs depending on the reaction mechanism with $^1O_2$. The trap-type RMs react with $^1O_2$ irreversibly, the singlet oxygen inactive RMs are comparatively less reactive with $^1O_2$, and finally the quencher-type RMs react with $^1O_2$ reversibly relaxing $^1O_2$ into $^3O_2$ through quenching mechanism. Moreover, the reaction of RMs with $^1O_2$ commonly depresses the Li_2O_2 decomposition kinetic.

evolved during cycling. Generally, trap-type RMs are prone to react with $^1O_2$ and their Li_2O_2 oxidation kinetics changed significantly. In accord, TMPD, TTF and MPT have moderate kinetics but after 48 hours of exposure to $^1O_2$, it decreased dramatically, reaching nearly zero current. The suppressed current of trap-type RMs after $^1O_2$ exposure implies that their Li_2O_2 oxidation ability is affected by $^1O_2$ and could lead to poor charging performance of these RMs in cells. Among trap-type RM^{exp}s, $TMPD^{exp}$ still exhibited some oxidation behavior at higher potentials even though. TMPD has comparatively high reactivity with $^1O_2$ (Fig. S9b†). This suggests that a reaction product of TMPD and $^1O_2$ still possesses an oxidation state capable of oxidizing Li_2O_2. Superficially, $TEMPO^{exp}$ has no significant changes compared to TEMPO as shown in CV and UV-Vis data (Fig. 1 and 2). However, the Li_2O_2 oxidation kinetics, more closely related to the function of RMs, was observed to be depressed (Fig. 3). This emphasizes the possibility again that $^1O_2$ can affect to RMs activity regardless of RM status by environmental change due to parasitic reaction of electrolyte and electrode with $^1O_2$. It is confirmed that reaction with $^1O_2$ differs depending on RMs. Certain RMs have a reversible quenching mechanism while others have severely irreversible trapping mechanisms with $^1O_2$ to extent of exhibiting no electrochemical activity. Even though RMs have different reactions with $^1O_2$, the chemical reactivity of all RMs with Li_2O_2 is significantly affected by $^1O_2$ (Fig. 4). What fundamentally regulates the cycle life of RMs in LOBs is how well RMs decompose Li_2O_2. Therefore, this discovery makes a point that controlling the $^1O_2$ will lead to highly cyclable RMs with sustained activity. It should be noted that the reaction with $^1O_2$ is the main focus in this work, however, the electrolyte stability towards other reactive oxygen species should not be ignored. To achieve highly stable LOBs, not just a single part, but effort with wider view point is still required.

Conclusion

Here we present chemical and electrochemical properties of RMs before and after exposure to $^1O_2$. The reactivity of each RM with $^1O_2$ differs depending on the molecular structure, as already reported, and can affect the chemical and electrochemical activity of RMs. Following the chemical behavior after exposure to $^1O_2$, RMs can be classified into trap-type, quencher-type, or singlet oxygen durable species. The trap-type RMs react with $^1O_2$ severely, losing their electrochemical activity and $^1O_2$ scavenging ability. The quencher-type RMs have a reversible reaction mechanism with $^1O_2$ relaxing into $^3O_2$ and exhibit well-sustained electrochemical activity. Lastly, the singlet oxygen durable species have no interaction with $^1O_2$ so that they have no scavenging behavior but less depressed electrochemical characteristics. However, the Li_2O_2 oxidation ability of RMs are considerably affected by $^1O_2$, even though certain RM showed quencher-type behavior. This indicates that $^1O_2$ is a concern for the life-span and managing the evolution of $^1O_2$ is an important approach to increase cyclability of RMs. From a practical point of view, not only the $^1O_2$ management but also the high stability of RM toward $^1O_2$ is important since $^1O_2$ evolution will follow the capacity increment and can trigger side reactions with solvent or other components of cell. Such that, using highly stable quencher-type RM can lead to fewer side reactions by electrolyte components and high cyclability of the cell. Moreover, the strategy documented here allows for the classification of RMs and enables an assessment for the stability and functionality of RMs which is important for the development of new RMs with high effectiveness and durability towards $^1O_2$.

Author contributions

H. W. L. and W. J. K. conceptualized and designed the experiments. H. W. L., J. Y. K. and J. E. K. synthesized materials and conducted cyclic voltammetry. J. Y. K., J. E. K. and Y. J. J. conducted kinetic measurements. H. W. L. and J. Y. K. conducted UV-Vis. H. W. L., D. D., X. Y. wrote original draft. X. G. and W. J. K. reviewed and edited the manuscript. X. G., P. G. B. and W. J. K. supervised the project.

Conflicts of interest

There are no conflicts to declare.

Acknowledgements

This work has been supported by the National Research Foundation of Korea (NRF) grant funded by the Korea government (MSIT) (No. 2021R1C1C1004598) and Basic Science Research Program through the National Research Foundation of Korea (NRF) funded by the Ministry of Education (No. NRF-2021R1A6A1A10044950). This research has also been supported by the POSCO Science Fellowship of POSCO TJ Park Foundation.

Notes and references

1 W.-J. Kwak, Rosy, D. Sharon, C. Xia, H. Kim, L. R. Johnson, P. G. Bruce, L. F. Nazar, Y.-K. Sun, A. A. Frimer, M. Noked, S. A. Freunberger and D. Aurbach, *Chem. Rev.*, 2020, **120**, 6626–6683.
2 M. Mirzaeian and P. J. Hall, *J. Power Sources*, 2010, **195**, 6817–6824.
3 U. Sahapatsombut, H. Cheng and K. Scott, *J. Power Sources*, 2013, **243**, 409–418.
4 J.-L. Shui, J. S. Okasinski, P. Kenesei, H. A. Dobbs, D. Zhao, J. D. Almer and D.-J. Liu, *Nat. Commun.*, 2013, **4**, 2255.
5 Y. Wang, Y.-R. Lu, C.-L. Dong and Y.-C. Lu, *ACS Energy Lett.*, 2020, **5**, 1355–1363.
6 D. Wang, F. Zhang, P. He and H. Zhou, *Angew. Chem.*, 2019, **131**, 2377–2381.
7 Z. Huang, J. Ren, W. Zhang, M. Xie, Y. Li, D. Sun, Y. Shen and Y. Huang, *Adv. Mater.*, 2018, **30**, 1803270.
8 X. Xin, K. Ito, A. Dutta and Y. Kubo, *Angew. Chem., Int. Ed.*, 2018, **57**, 13206–13210.
9 G. Li, N. Li, S. Peng, B. He, J. Wang, Y. Du, W. Zhang, K. Han and F. Dang, *Adv. Energy Mater.*, 2021, **11**, 2002721.

10 H. Hou, Y. Cong, Q. Zhu, Z. Geng, X. Wang, Z. Shao, X. Wu, K. Huang and S. Feng, *Chem. Eng. J.*, 2022, **448**, 137684.
11 H. Song, S. Xu, Y. Li, J. Dai, A. Gong, M. Zhu, C. Zhu, C. Chen, Y. Chen, Y. Yao, B. Liu, J. Song, G. Pastel and L. Hu, *Adv. Energy Mater.*, 2018, **8**, 1701203.
12 Y. Wu, X. Zhu, W. Wan, Z. Man, Y. Wang and Z. Lü, *Adv. Funct. Mater.*, 2021, **31**, 2105664.
13 X. Chen, L. Qin, J. Sun, S. Zhang, D. Xiao and Y. Wu, *Angew. Chem., Int. Ed.*, 2022, **61**(33), e202207018.
14 C.-L. Li, G. Huang, Y. Yu, Q. Xiong, J.-M. Yan and X. Zhang, *J. Am. Chem. Soc.*, 2022, **144**, 5827–5833.
15 B. J. Bergner, A. Schürmann, K. Peppler, A. Garsuch and J. Janek, *J. Am. Chem. Soc.*, 2014, **136**, 15054–15064.
16 D. Kundu, R. Black, B. Adams and L. F. Nazar, *ACS Cent. Sci.*, 2015, **1**, 510–515.
17 Z. Liang and Y.-C. Lu, *J. Am. Chem. Soc.*, 2016, **138**, 7574–7583.
18 W. Yu, X. Wu, S. Liu, H. Nishihara, L. Li and C.-W. Nan, *Energy Storage Mater.*, 2021, **38**, 571–580.
19 J. Kim, J. Jeong, G. Y. Jung, J. Lee, J. E. Lee, K. Baek, S. J. Kang, S. K. Kwak, C. Hwang and H.-K. Song, *ACS Appl. Mater. Interfaces*, 2022, **14**, 40793–40800.
20 Y. Chen, S. A. Freunberger, Z. Peng, O. Fontaine and P. G. Bruce, *Nat. Chem.*, 2013, **5**, 489–494.
21 J. Wandt, P. Jakes, J. Granwehr, H. A. Gasteiger and R.-A. Eichel, *Angew. Chem.*, 2016, **128**, 7006–7009.
22 D. Zhai, H.-H. Wang, J. Yang, K. C. Lau, K. Li, K. Amine and L. A. Curtiss, *J. Am. Chem. Soc.*, 2013, **135**, 15364–15372.
23 G. Houchins, V. Pande and V. Viswanathan, *ACS Energy Lett.*, 2020, **5**, 1893–1899.
24 J. Kim, H. Lee and W. Kwak, *Adv. Funct. Mater.*, 2022, **32**, 2209012.
25 Z. Liang, Y. Zhou and Y.-C. Lu, *Energy Environ. Sci.*, 2018, **11**, 3500–3510.
26 A. T. S. Freiberg, M. K. Roos, J. Wandt, R. de Vivie-Riedle and H. A. Gasteiger, *J. Phys. Chem. A*, 2018, **122**, 8828–8839.
27 W.-J. Kwak, H. Kim, Y. K. Petit, C. Leypold, T. T. Nguyen, N. Mahne, P. Redfern, L. A. Curtiss, H.-G. Jung, S. M. Borisov, S. A. Freunberger and Y.-K. Sun, *Nat. Commun.*, 2019, **10**, 1380.
28 N. Mahne, B. Schafzahl, C. Leypold, M. Leypold, S. Grumm, A. Leitgeb, G. A. Strohmeier, M. Wilkening, O. Fontaine, D. Kramer, C. Slugovc, S. M. Borisov and S. A. Freunberger, *Nat. Energy*, 2017, **2**, 17036.
29 S. Dong, S. Yang, Y. Chen, C. Kuss, G. Cui, L. R. Johnson, X. Gao and P. G. Bruce, *Joule*, 2022, **6**, 185–192.
30 J. Wandt, A. T. S. Freiberg, A. Ogrodnik and H. A. Gasteiger, *Mater. Today*, 2018, **21**, 825–833.
31 N. Mahne, S. E. Renfrew, B. D. McCloskey and S. A. Freunberger, *Angew. Chem., Int. Ed.*, 2018, **57**, 5529–5533.
32 Z. Liang, Q. Zou, J. Xie and Y.-C. Lu, *Energy Environ. Sci.*, 2020, **13**, 2870–2877.
33 Y. K. Petit, E. Mourad, C. Prehal, C. Leypold, A. Windischbacher, D. Mijailovic, C. Slugovc, S. M. Borisov, E. Zojer, S. Brutti, O. Fontaine and S. A. Freunberger, *Nat. Chem.*, 2021, **13**, 465–471.
34 H. Lee, H. Kim, H. Jung, Y. Sun and W. Kwak, *Adv. Funct. Mater.*, 2021, **31**, 2102442.
35 W.-J. Kwak, J. Park, H. Kim, J. M. Joo, D. Aurbach, H. R. Byon and Y.-K. Sun, *ACS Energy Lett.*, 2020, **5**, 2122–2129.
36 P. P. Bawol, P. Reinsberg, C. J. Bondue, A. A. Abd-El-Latif, P. Königshoven and H. Baltruschat, *Phys. Chem. Chem. Phys.*, 2018, **20**, 21447–21456.
37 M. Kořinek, R. Dědic, A. Svoboda and J. Hála, *J. Fluoresc.*, 2004, **14**, 71–74.
38 J. A. S. Cavaleiro, H. Görner, P. S. S. Lacerda, J. G. MacDonald, G. Mark, M. G. P. M. S. Neves, R. S. Nohr, H.-P. Schuchmann, C. von Sonntag and A. C. Tomé, *J. Photochem. Photobiol., A*, 2001, **144**, 131–140.
39 Y. Hao, B. M. Liu, T. F. Bennett, C. G. Monsour, M. Selke and Y. Liu, *J. Phys. Chem. C*, 2021, **125**, 7392–7400.
40 E. J. Corey and W. C. Taylor, *J. Am. Chem. Soc.*, 1964, **86**, 3881–3882.
41 D. Córdoba, H. B. Rodríguez and E. J. Calvo, *ChemistrySelect*, 2019, **4**, 12304–12307.
42 Z. Jiang, Y. Huang, Z. Zhu, S. Gao, Q. Lv and F. Li, *Proc. Natl. Acad. Sci.*, 2022, **119**, 6–11.
43 E. Gross, B. Ehrenberg and F. M. Johnson, *Photochem. Photobiol.*, 1993, **57**, 808–813.
44 F. Jensen, A. Greer and E. L. Clennan, *J. Am. Chem. Soc.*, 1998, **120**, 4439–4449.
45 C. Ye, Y. Zhang, A. Ding, Y. Hu and H. Guo, *Sci. Rep.*, 2018, **8**, 2205.
46 J. J. Liang, C. L. Gu, M. L. Kacher and C. S. Foote, *J. Am. Chem. Soc.*, 1983, **105**, 4717–4721.
47 A. P. Darmanyan, W. S. Jenks and P. Jardon, *J. Phys. Chem. A*, 1998, **102**, 7420–7426.
48 Y. Ko, H. Park, B. Lee, Y. Bae, S. K. Park and K. Kang, *J. Mater. Chem. A*, 2019, **7**, 6491–6498.

